91602
new 82-10

LEGAL NOTICE

This report was prepared by Ontario Hydro and, while effort has been made to assure the accuracy and applicability of the material contained herein, neither Ontario Hydro nor any person acting on its behalf:

(a) makes any warranty, express or implied with respect to the use of any information, apparatus, method or process disclosed in this report or that such use may not intringe privately owned rights; or

(b) assumes any liabilities with respect to the use of, or for damages resulting from the use of, any information, apparatus, method or process disclosed in this report.

ontario hydro
research division
COMPLIMENTARY COPY
Please Credit Ontario Hydro Research if Reproduced in Whole or in Part

DEVELOPMENT OF GAMMA SPECTROMETRY SYSTEM FOR IN-SITU MEASUREMENT OF RADIOACTIVITY WITHIN PIPING

Report No. 88-227-K

A. Husain - Engineer
Materials Chemistry Section
Chemical Research Department

ABSTRACT

A gamma spectrometer system was developed for in-situ measurement of radioactivity within feeder pipes located in the feeder cabinets at Pickering and Bruce. Appropriate shielding was devised from a consideration of the relatively high radiation fields and multiplicity of extraneous sources at the measurement location. The shielded spectrometer system was subsequently evaluated in the field. To interpret data, the energy and distance dependence of the detector's efficiency was measured for a pipe source with surface or volumetric activity and compared with model predictions. It was shown that the efficiencies could be used to determine the surface and/or volume contributions to the total activity of a pipe. In-situ measurements of active pipe sections compared reasonably well with direct assay of appropriate specimens from the pipe sections.

job	file	date	report no.
32-600-200	836.3332	November 28, 1988	88-227-K

91602
new 82-10

ontario hydro
research division

EXECUTIVE SUMMARY

DEVELOPMENT OF A GAMMA SPECTROMETRY SYSTEM FOR IN-SITU MEASUREMENT OF RADIOACTIVITY WITHIN PIPING

A. Husain
Materials Chemistry Section
Chemical Research Dept

The deposition of activated corrosion and fission products on reactor out-core primary heat transport (PHT) system surfaces leads to growth of gamma radiation fields around piping and other system components. For the purposes of monitoring radiation field growth and decontamination planning, in-situ gamma spectrometry of PHT system components is routinely conducted at Ontario Hydro's nuclear reactors. A portable hyperpure germanium gamma spectroscopy system is used to determine the contribution of various radioisotopes to radiation fields outside a number of components.

Aside from the composition of radiation fields, the inventory of radioisotopes within the components is also of interest. Previous work from AECL has examined the relationship between measured boiler fields and the activity of Co-60 within a boiler. This approach, however cannot be used when a number of isotopes contribute significantly to the field; in-situ gamma spectrometry can instead be applied.

The development of in-situ gamm spectrometry to measure radioisotope activities within feeder pipes was initiated in 1985 as part of an overall thrust to develop measurement capabilities for various PHT system components such as piping, end fittings, boilers, etc. The feeders collectively represent, next to the boilers, the second largest surface area in the PHT system. A capability to measure activity levels within feeder pipes is useful for the following reasons:

1) in previous PHT system decontaminations, measurement of the specific activity of the oxide prior to the decontamination necessitated the removal of feeder pipe sections from the system; in-situ measurement of activity and oxide thickness (ultrasonic techniques may be applicable) will make this expensive procedure unnecessary,

job	file	date	report no.
32-600-200	836.3332	November 28, 1988	88-227-K

2) the transport of activity in general and in particular that of Sb-124 during and after a PHT system decontamination can be more readily understood, and

3) shielding requirements for a decontamination rig can be better defined.

This report describes the work undertaken to develop in-situ gamma spectrometry for measuring the activity of radioisotopes within feeder pipes located in the feeder cabinets at Pickering and Bruce. Appropriate uranium metal shielding was devised from a consideration of the relatively high radiation fields and multiplicity of extraneous sources at the measurement location. The shielded spectrometer system was subsequently evaluated in the field. To interpret spectra, the energy and distance dependence of the detector's efficiency was measured for a pipe source with surface or volumetric activity and compared with model predictions. It was shown that the efficiencies could be used to determine the surface and/or volume contributions to the total activity of a pipe. In-situ measurements of active pipe sections compared reasonably well with direct assay of appropriate specimens from the pipe sections.

Although the spectrometer system functioned as expected during field evaluations, ie, source counts were distinguished from background counts in fields as high as 100 mR/h, it would be preferable for ease of spectra interpretation to replace the uranium shield (contributes spectral interferences) with one fabricated to the same specifications from tungsten alloy. The lower weight of the tungsten shield would contribute to increased portability and despite its lower attenuation, the shield would still be adequate for its intended service.

Additional measurements including radiation field measurements using a shielded gamma survey probe, are required to validate the proposed technique for determining feeder pipe activity. A reasonable agreement between measured radiation fields and those calculated from the measured activities would be expected.

TABLE OF CONTENTS

		Page
1.0	INTRODUCTION AND BACKGROUND	1
2.0	CONFIGURATION OF FEEDER PIPES	2
3.0	SHIELDING CONSIDERATIONS	4
4.0	DETECTOR EFFICIENCY FOR PIPE SOURCES - EXPERIMENTAL SYSTEM	7
5.0	RELATIONSHIP BETWEEN PIPE AND POINT SOURCE EFFICIENCIES	13
6.0	PIPE SOURCE EFFICIENCY - RESULTS AND DISCUSSION	15
	6.1 Surface Activity	15
	6.2 Volumetric Activity	17
	6.3 Surface and Volumetric Activity	23
	6.4 Pipe Source Efficiency Calibration - Lead vs. Uranium Detector Shield	28
7.0	MEASUREMENT OF PIPE ACTIVITY - FEEDER PIPE SECTIONS	28
8.0	MEASUREMENT OF PIPE ACTIVITY IN FEEDER CABINET	31
9.0	SUMMARY, CONCLUSIONS AND RECOMMENDATIONS	33
ACKNOWLEDGEMENT		34
REFERENCES		35
DISTRIBUTION		last page

LIST OF TABLES

Table		Page
1	SLAB SHIELD REQUIRED TO OBTAIN AN ATTENUATION FACTOR OF 250	4
2	ACTIVITY OF SOURCE SHEET	10
3	DIMENSIONS OF COLLIMATORS USED	15
4	RESULTS OF A TYPICAL PIPE EFFICIENCY MEASUREMENT	16
5	MEASURED EFFICIENCIES FOR PIPE SOURCE	27
6	KNOWN ACTIVITIES OF PIPE SOURCE	27
7	ESTIMATED ACTIVITIES OF PIPE SOURCE	27
8	ACTIVE FEEDER PIPES EXAMINED	28
9	ACTIVITY OF FEEDER PIPES - METHODS 1 AND 2 COMPARED	30
10	MEASURED ACTIVITIES OF OUTLET FEEDERS IN PNGS UNIT 6	32

LIST OF FIGURES

Figure		Page
1	SCHEMATIC OF THE FEEDER CABINETS AT BRUCE	3
2	TYPICAL END-VIEW OF A HEADER INDICATING THE LOCATIONS WHERE FEEDER PIPES ARE CONNECTED TO IT	3
3	TYPICAL DISTRIBUTION OF FEEDER PIPES - A VIEW OF THE HEADER AS SEEN FROM BELOW	3
4	A VIEW INSIDE THE FEEDER CABINET AT BRUCE	5
5	SIMPLIFIED ILLUSTRATION OF THE PORTABLE GAMMA SPECTROMETER SYSTEM	6
6	THE TWO HALVES OF THE ANNULAR SHIELD	8
7	COLLIMATORS AND CYLINDRICAL PLUGS	8
8	THE PIPE-DETECTOR GEOMETRY	9
9	PLACEMENT OF SOURCE SHEET DURING CALIBRATION	11
10	THE EXPERIMENTAL SYSTEM FOR MEASURING PIPE SOURCE EFFICIENCY	12
11	ENERGY DEPENDENCE OF PIPE (SURFACE ACTIVITY) AND POINT SOURCE EFFICIENCIES - PIPE 1	18
12	ENERGY DEPENDENCE OF PIPE (SURFACE ACTIVITY) AND POINT SOURCE EFFICIENCIES - PIPE 2	19
13	DISTANCE DEPENDENCE OF THE PIPE (SURFACE ACTIVITY) SOURCE EFFICIENCY	20
14	VARIATION WITH DISTANCE OF THE RATIO OF THE MEASURED PIPE SOURCE (SURFACE ACTIVITY) EFFICIENCY TO THAT CALCULATED BASED ON EQN. [3]	21
15	ENERGY DEPENDENCE OF PIPE (VOLUMETRIC ACTIVITY) AND POINT SOURCE EFFICIENCIES	22
16	DISTANCE DEPENDENCE OF THE PIPE (VOLUMETRIC ACTIVITY) SOURCE EFFICIENCY	24
17	VARIATION WITH DISTANCE OF THE RATIO OF THE MEASURED PIPE SOURCE (VOLUMETRIC ACTIVITY) EFFICIENCY TO THAT CALCULATED BASED ON EQN. [7]	25
18	DISTANCE DEPENDENCE OF SURFACE AND VOLUME SOURCE EFFICIENCIES	26
19	COMPARISON OF PIPE SOURCE (SURFACE ACTIVITY) EFFICIENCIES - LEAD VS. URANIUM DETECTOR SHIELD	29

91601
new 82-10

ontario hydro
research division

To Dr. D. Mills
Director of Research

DEVELOPMENT OF A GAMMA SPECTROMETRY SYSTEM FOR IN-SITU MEASUREMENT OF RADIOACTIVITY WITHIN PIPING

1.0 INTRODUCTION AND BACKGROUND

The deposition of activated corrosion and fission products on reactor out-core primary heat transport (PHT) system surfaces leads to growth of gamma radiation fields around piping and other system components. Activated corrosion products arise from the corrosion of system materials which release oxidation products to the circulating coolant either as dissolved metal ions or as particulate/colloidal metal oxides. Transportation and deposition of these products in-core, their subsequent activation in the neutron flux and re-entry of the activated products into the coolant results in contamination of the out-core surfaces. Among the principal radioisotopes produced by activation, namely, Co-60, Zr/Nb-95, Cr-51, Fe-59, Mn-54, Zn-65 etc, the dominant contributor to out-core radiation fields is generally Co-60. On the other hand, fission products on out-core surfaces arise from transport out of core of fission isotopes which have escaped due to breaches in the fuel element cladding. The principal gamma-emitting fission radionuclides generally observed on out-core surfaces include Zr/Nb-95 and Ba/La-140.

The out-core radioactive deposits are responsible for the significant radiation exposure to personnel undertaking inspection and maintenance tasks during reactor shutdown. For the purposes of monitoring radiation field growth and decontamination planning, in-situ gamma spectrometry of PHT system components is routinely conducted at Ontario Hydro's nuclear reactors. A portable hyperpure germanium gamma spectroscopy system is used to determine the contribution of various radioisotopes to radiation fields outside a number of components/1,2/.

Aside from the composition of radiation fields, the inventory of radioisotopes within the components is also of interest. Unpublished work/3,4/ in the 1970's from Atomic Energy of Canada Ltd. examined the relationship between measured boiler fields and the activity of Co-60 within a boiler.

This approach cannot be used when a number of isotopes contribute significantly to the field; in-situ gamma spectrometry can instead be applied to determine their activity levels as demonstrated by Palino/5/ and Harvill et al/6/.

The development of in-situ gamma spectrometry to measure radioisotope activities within feeder pipes was initiated in 1985 as part of an overall thrust to develop measurement capabilities for various PHT system components such as piping, end fittings, boilers, etc. The feeders collectively represent, next to the boilers, the second largest surface area in the PHT system. A capability to measure activity levels within feeder pipes is useful for the following reasons:

1) in previous PHT system decontaminations, measurement of the specific activity of the oxide prior to the decontamination necessitated the removal of feeder pipe sections from the system; in-situ measurement of activity and oxide thickness (ultrasonic techniques may be applicable) will make this expensive procedure unnecessary,

2) the transport of activity in general and in particular that of Sb-124 during and after a PHT system decontamination can be more readily understood, and

3) shielding requirements for a decontamination rig can be better defined.

This report describes the work undertaken to develop in-situ gamma spectrometry for measuring the activity of radioisotopes within feeder pipes. This work included the design and fabrication of appropriate shielding, a laboratory calibration program to measure detector efficiencies for various pipe-detector geometries, comparison of measured efficiencies with model predictions, verification of developed procedures and field measurements.

2.0 CONFIGURATION OF FEEDER PIPES

Ontario Hydro's CANDU reactors typically have several hundred horizontal fuel channels housing the natural uranium fuel. The heavy water coolant flows into a fuel channel through an inlet feeder pipe and exits at its other end through an outlet feeder pipe. The inlet and outlet feeders rise several meters above the reactor face to merge into the inlet and outlet headers, respectively. The outlet headers transport the hot coolant to the boilers; the heat-exchanged coolant, thereafter, returns to the reactor via the inlet headers.

Figure 1 shows the arrangement at Bruce of the headers housed inside the horizontal feeder cabinet. At Pickering, there is only one inlet and one outlet header at each end of the reactor; each header is, however, in two separate sections corresponding to the North and South loops of the PHT system. The typical end-view of a header pipe is shown in Figure 2 and indicates the locations where feeder pipes are joined to it. The distribution of feeder pipes along a header (corresponding to locations A-E in Figure 2) is schematically shown in Figure 3. Although the feeders for simplicity

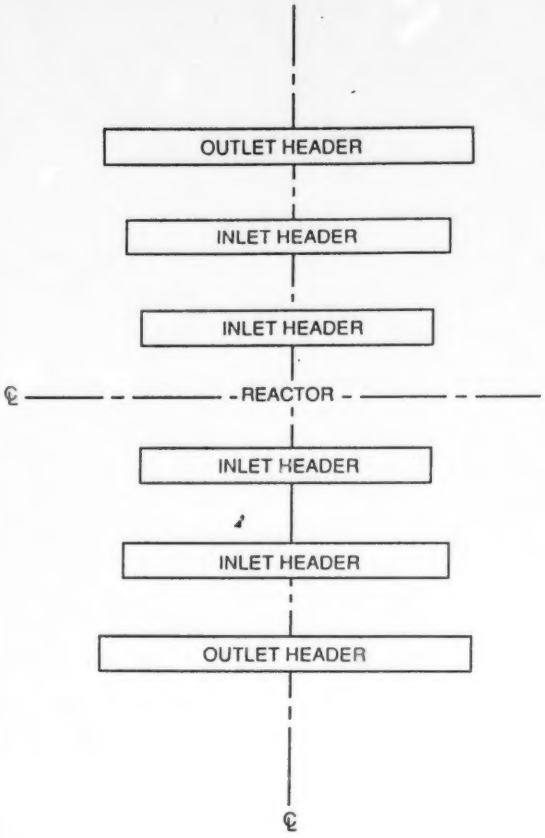

FIGURE 1

SCHEMATIC OF THE FEEDER CABINETS AT BRUCE

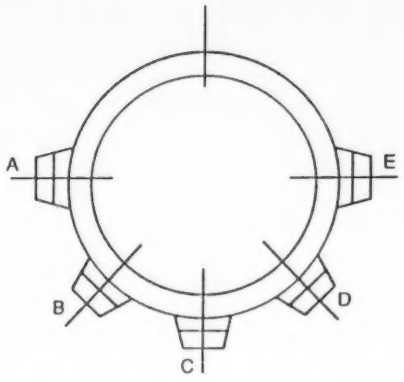

FIGURE 2

TYPICAL END-VIEW OF A HEADER INDICATING THE LOCATIONS WHERE FEEDER PIPES ARE CONNECTED TO IT

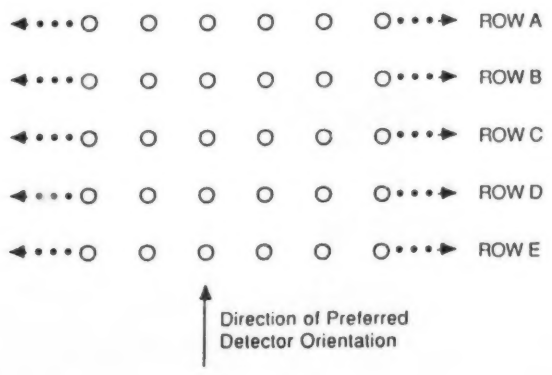

FIGURE 3

TYPICAL DISTRIBUTION OF FEEDER PIPES -
A VIEW OF THE HEADER AS SEEN FROM BELOW

are indicated with equi-sized circles, in general, their size varies across each row and between rows. Additionally, pipes may not be present at some locations. The distance between adjacent pipes along a row or between rows is typically less than or equal to ~30cm.

3.0 SHIELDING CONSIDERATIONS

A view inside the feeder cabinet at Bruce is shown in Figure 4. It illustrates the multiplicity of extraneous radioactive sources and the spatial complexity involved in performing in-situ spectrometry of a feeder pipe. Radiation fields inside the feeder cabinet may typically exceed 100 mR/h. With the spectrometer positioned on the walkway (less than 60 cm wide and about 120 cm below the cabinet ceiling) so that it points at the pipe of interest, radiation reaches the detector practically from all directions. The detector, therefore, has to be appropriately shielded and collimated to significantly reduce the background radiation.

Figure 5 shows the portable gamma spectrometer system (manufactured by Aptec Engineering Ltd.) used for ongoing measurements at the nuclear stations. The planar germanium detector housing is shielded along its length by an annular lead shield of thickness ~4.5 cm, at the back by 2.5 cm of tungsten alloy and at the front by a lead collimator of length 6.35 cm. These shield thicknesses correspond, respectively, to 5.5, 7.6 and 1.7% transmissions for 1332 KeV gamma photons. In addition to the tungsten back shield, radiation from behind is also attenuated (by ~45% for Co-60 radiation) by the filled liquid nitrogen dewar.

While the shielding described above is adequate for routine spectrometry in support of the radiation field monitoring program at Ontario Hydro, it is inadequate for measurements of feeder pipe activity. Based on earlier exploratory experience and Palino's work/5/ a shield thickness sufficient to attenuate Co-60 radiation by a factor of 250 is required. From a comparison of the shielding materials in Table 1, it is evident that a uranium shield would be the most compact and weigh the least compared with a lead or

TABLE 1

SLAB SHIELD REQUIRED TO
OBTAIN AN ATTENUATION FACTOR OF 250

Energy (MeV)	Shield Thickness (cm)			Wt. of Shield* (g)		
	Lead	Tungsten	Uranium	Lead	Tungsten	Uranium
1.0	7.1	4.8	3.7	80.2	86.7	71.1
1.5	9.6	5.9	5.3	108.5	113.4	100.8

* Corresponding to a 1x1 cm^2 slab with the specified shield thickness.

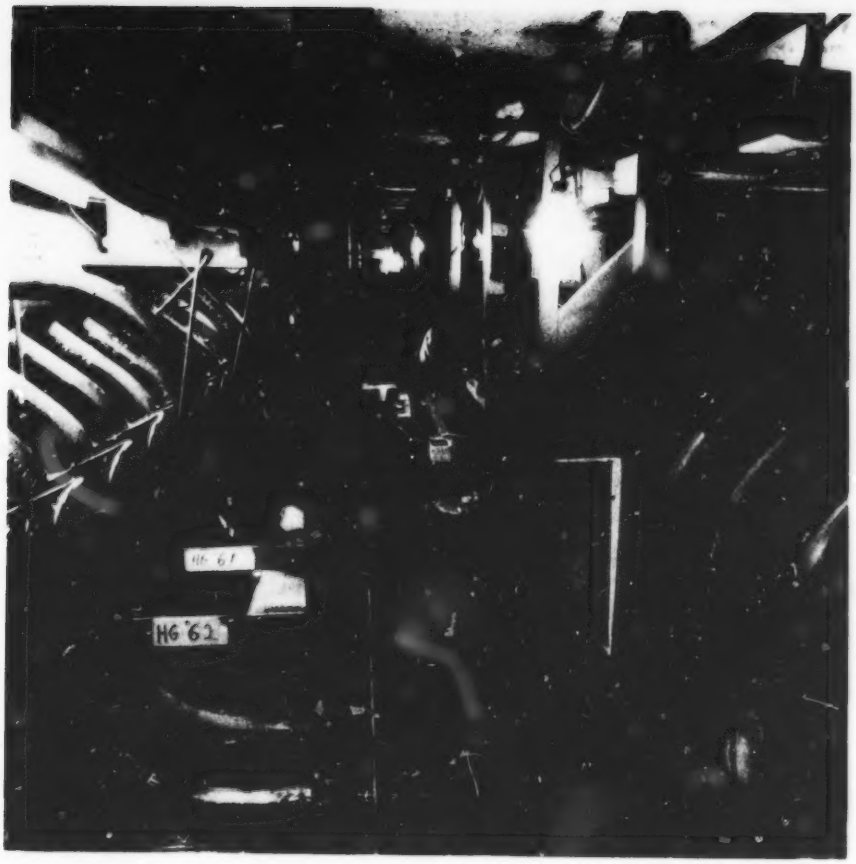

FIGURE 4

A VIEW INSIDE THE FEEDER CABINET AT BRUCE

178079 RD
CAZ-4

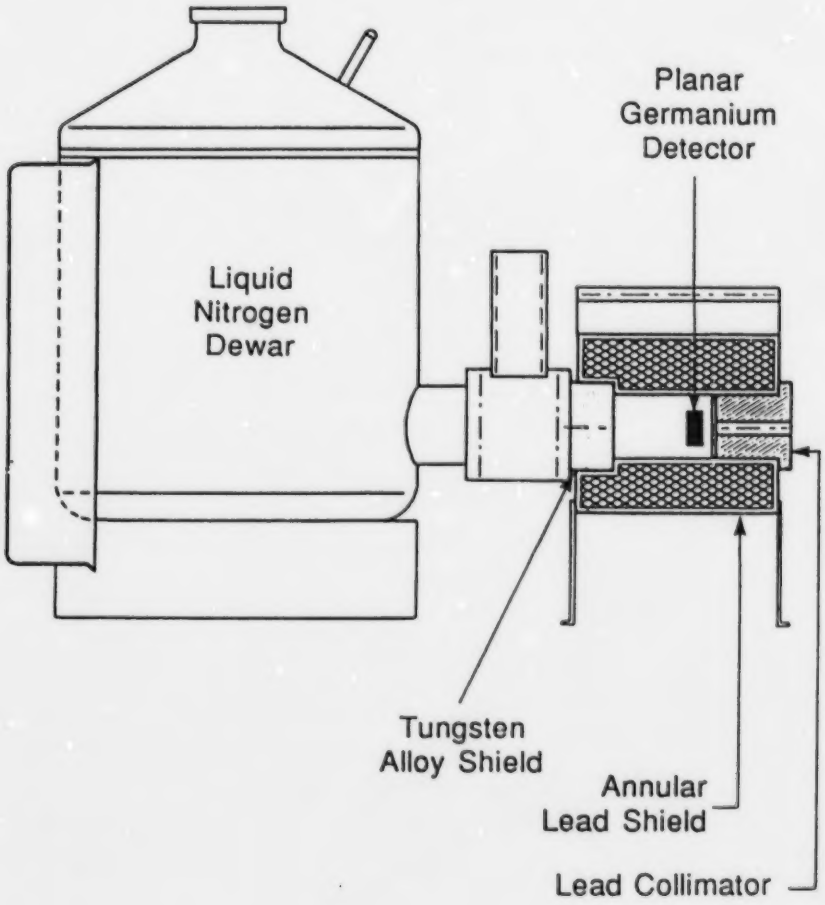

FIGURE 5

SIMPLIFIED ILLUSTRATION OF THE PORTABLE GAMMA SPECTROMETER SYSTEM

tungsten shield (attenuation coefficients taken from Ref. 7). The inherent radioactivity of a uranium shield should, however, be recognized.

Accordingly, an annular shield was designed and fabricated (jointly by Eldorado Resources Ltd and Leavens Aviation) from depleted uranium metal; a tungsten alloy sleeve (supplied by Teledyne Powder Alloys (97% W)) was shrink-fitted inside the central bore to shield the detector from the field associated with the uranium. For portability, the shield was made in two cylindrical sections (each weighing about 30 kgs) with their mating surfaces behind the plane of the detector (when the shield is positioned over the detector housing) and stepped to prevent radiation streaming. The outer shield surfaces were encased in stainless steel while all exposed internal uranium surfaces were nickel-plated. The shield, shown in Figure 6, has an overall length and diameter of 15 cm and 17 cm, respectively.

Collimators and cylindrical plugs to fit inside the collimator holes were for simplicity fabricated from lead (by Canada Metals). These are shown in Figure 7.

The extent of shielding at the back of the detector has previously been noted. The annular shield when in place also serves to collimate the detector from radiation entering from behind. Because of the uncertainty in additional back shielding requirements for the feeder pipe measurements, the use of lead blankets was considered until needs could be better defined.

Consider the shielded detector system positioned perpendicularly across the walkway and viewing a feeder pipe. As long as the detector's field of view excludes pipes in adjacent pipe banks (columns in Figure 3), the detector will receive radiation only from the pipe being scanned and from all those behind it in the same bank. The more distant a pipe is in a bank, the greater is the portion of its length viewed. The increased contribution is, however, offset by the greater attenuation due to the intervening metal (pipe wall) and water (inside pipe) thicknesses. For typical field geometries where the projected diameter P (see Figure 8) is less than or equal to the OD of the pipe, the interference from pipes in the same bank can effectively be minimised by using a circular slab shield of diameter equal to the pipe's OD and placed behind the pipe. Accordingly, a circular pipe shield was made from depleted uranium and encased in stainless steel. It has a diameter of ~13 cm and a thickness of ~6 cm.

4.0 DETECTOR EFFICIENCY FOR PIPE SOURCES - EXPERIMENTAL SYSTEM

The interpretation of spectra requires the efficiency of the detector to be measured as a function of distance (between pipe and collimator face), pipe diameter, and collimator length and diameter. A feeder pipe with surface activity was simulated by wrapping a source sheet (see below) around a water-filled plexiglass tube which was then placed concentrically inside the pipe. Radioactivity was introduced into the water to simulate a volumetric pipe source. Combinations of pipe and tube were chosen so as to minimize the air gap between them without inconveniencing the positioning of the source sheet.

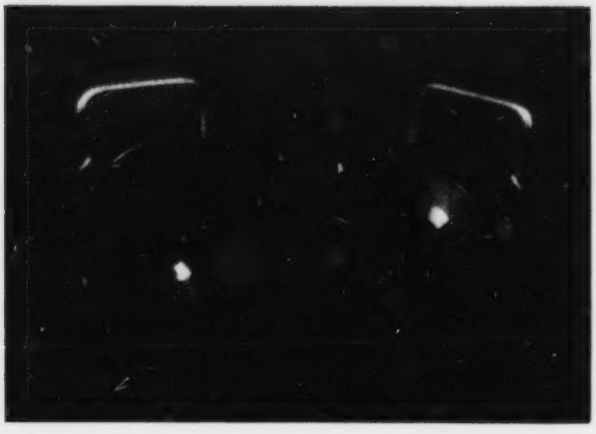

FIGURE 6

THE TWO HALVES OF THE ANNULAR SHIELD

FIGURE 7

COLLIMATORS AND CYLINDRICAL PLUGS -
COLLIMATOR NO'S. 2-4 (LEFT), COLLIMATOR NO. 6 (RIGHT)

178081 RD
CAZ-4

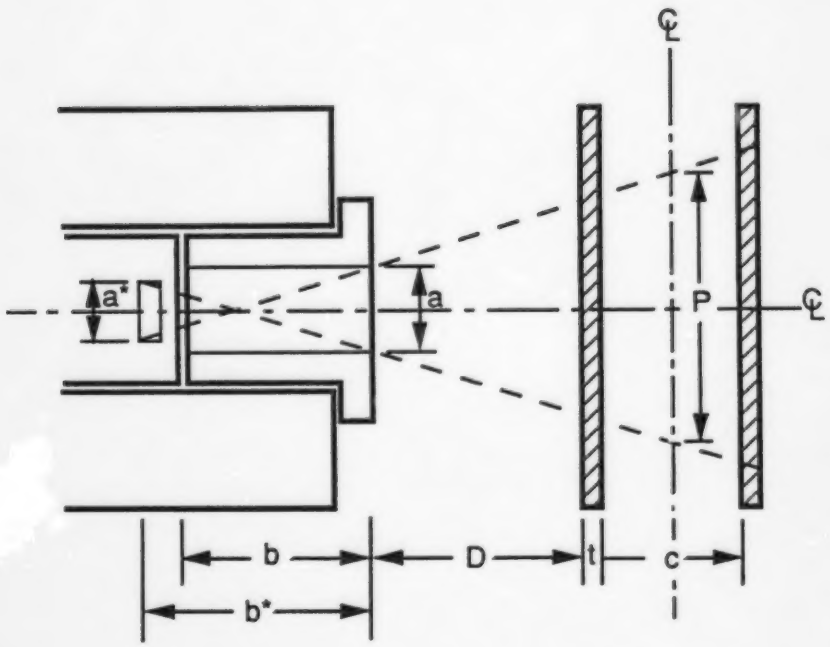

FIGURE 8

THE PIPE-DETECTOR GEOMETRY

The source sheet was prepared from a 15x25 cm strip of blotting paper. A 1x1 cm grid was drawn on one side of the paper while the other side was covered with adhesive tape. Small aliquots (50 µL) of a solution containing Ce-139, Sn-113, Cs-137, Y-88 and Co-60 were pipetted onto the center of each square in the grid. The top surface after drying was also covered in adhesive tape. The sheet was cut along its 25 cm length into suitable strips such that their appropriate combinations covered a 15 cm length of any of the plexiglass tubes selected. The activity deposited is shown in Table 2. Even though the sheet has discrete spots of activity on it, it has been shown /5/ to appear to the detector even at short distances (less than 1 cm) as being uniformly smeared.

TABLE 2

ACTIVITY OF SOURCE SHEET

Isotope	Activity* ($\mu Ci/cm^2$)
Ce-139	0.0328 ± 0.0008
Sn-113	0.1106 ± 0.0020
Cs-137	0.1270 ± 0.0030
Y-88	0.1176 ± 0.0024
Co-60	0.3650 ± 0.0090

* Measured on August 28, 1986

The calibration procedure involved two measurements at each position of the source sheet (see Figure 9), the first with the collimator hole open and the second with the hole plugged to determine background counts. For the pipe-detector distances considered, measurements with the source sheet beyond Position 2 were not necessary. Each set of measurements yielded the net peak counts for the various isotopes in the source. The total (Positions 1 and 2) net counts multiplied by 2 and corrected for the additional shielding due to a completely water-filled pipe (in the experimental system, an air gap exists between the pipe ID and the tube OD) represented the peak counts due to an extended pipe source located centrally about the collimator axis. The detector efficiency was then estimated from the known source activity.

The solution used for simulating a volumetric pipe source contained 0.133 µCi/ml Cs-137 and 0.257 µCi/ml Co-60 (activities as on December 12, 1987). The solution was filled to a height of 15 cm inside the tube. For this geometry, the pipe was first counted (Position 1) with the bottom of the tube lifted to the level of the collimator's axis. The second count (Position 2) was performed by elevating the tube by an additional 15 cm.

The experimental system is illustrated in Figure 10.

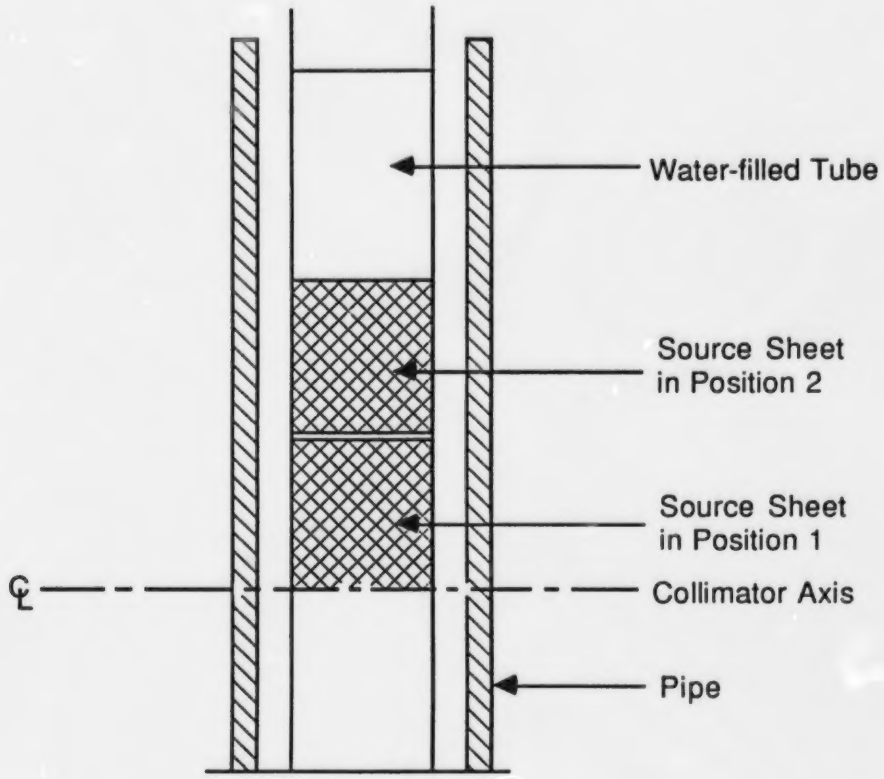

FIGURE 9

PLACEMENT OF SOURCE SHEET DURING CALIBRATION

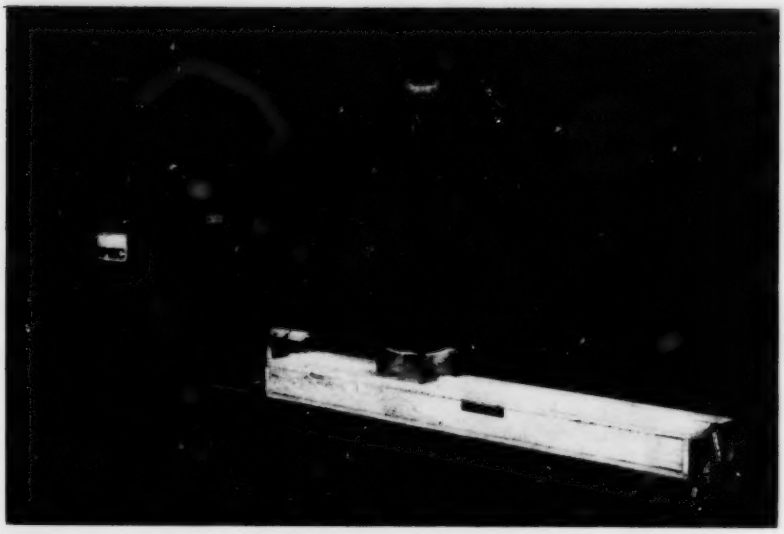

FIGURE 10

THE EXPERIMENTAL SYSTEM FOR MEASURING PIPE SOURCE EFFICIENCY

5.0 RELATIONSHIP BETWEEN PIPE AND POINT SOURCE EFFICIENCIES

A pipe with surface activity may be considered as a system of parallel plates with a separation equal to the pipe's ID and having uniformly smeared activity on the inside plate surfaces/5/. The parallel plate assumption leads to the following expression relating pipe and point source efficiencies:

$$\varepsilon(E)=\varepsilon_p(E)\frac{\pi a^2}{4} e^{-\mu t} (1+e^{-\mu_m c})(1-e^{-\mu_c b}) \frac{P_{e(E)}}{P_p(E)} \qquad [1]$$

$\varepsilon(E), \varepsilon_p(E)$ are the energy dependent pipe and point source efficiencies,

a is the diameter of the collimator hole,

b is the length of the collimator hole,

c is the plate spacing or pipe ID,

t is the pipe wall thickness,

$e^{-\mu t}$ is the attenuation due to the pipe wall (μ is the attenuation coefficient of the pipe material),

$e^{-\mu_m c}$ is the attenuation due to the medium (water) in the pipe (μ_m is the attenuation coefficient of the medium),

$(1-e^{-\mu_c b})$ is a factor arising from the consideration that the detector's response with the collimator hole open equals a background count X and a source count Y; with the hole plugged, the response is $X + Y\, e^{-\mu_c b}$ (μ_c is the attenuation coefficient of the collimator material),

$P_e(E), P_p(E)$ are the extended and point source penetration factors, respectively, accounting for the increase in gamma photons reaching the detector due to transmission through the collimator material.

The parallel plate approximation is valid for small pipe-collimator distances where the geometric projection of the collimator on the plane through the pipe's axis is less than or equal to its ID. For a collimator hole larger in diameter than the detector, the projection is given by $a^*\{ab^*/a^*+(2D+OD)(a+a^*)/2a^*\}/b^*$ (notation given in Figure 8); when the hole is smaller than the diameter of the detector, the expression reduces to $a(b+2D+OD)/b$. The limiting D for applicability of the parallel plate model is defined by the ratio R=Projection/ID equal to unity.

The ratio P_e/P_p can be estimated/8/ from the expression

$$P_e(E)/P_p(E) = \{(\mu_c b-1)/(\mu_c b-2)\}^2 \qquad [2]$$

which is valid for a detector that is much larger than the hole in the collimator and for a position-independent interaction response within the detector. Otherwise, the ratio is determined by measuring the efficiency of an extended planar source and applying Eqn.[1] considering the term $e^{-\mu t}(1 + e^{-\mu_m c})$ equal to unity.

Polyakov and Chechetkin /9/ also have derived expressions for a pipe source assuming in one case (small D, $(b+D)<bc/a$) a parallel plate and in the other case (large D, $(b+D)<bc/a$) a line source geometry. Their expression for the first case is essentially identical to Eqn. [1] with $P_e(E)/P_p(E)$ given by $\{1 + 4/(\mu_c b) + 4/(\mu_c b)^2\}$. The line source assumption led to the expression

$$\varepsilon(E)=\varepsilon_\ell(E)\frac{\pi c}{2}\, e^{-\mu t}(1+e^{-\mu_m c})\,(1-e^{-\mu_c b})\, P_\ell(E) \qquad [3]$$

where ε_ℓ (E) and P_ℓ (E), the line source efficiency and penetration factor are, respectively, given by

$$\varepsilon_\ell(E) = \varepsilon_p(E)\,\frac{ab}{(b+D)} \qquad [4]$$

$$P_\ell(E) = \left\{1+\frac{3}{\mu_c\sqrt{b(b+D)}} + \frac{3}{\mu_c^2 b(b+D)}\right\} \qquad [5]$$

Polyakov and Chechetkin have also derived expressions for a volumetric pipe source. For the two cases of small and large D, these are respectively, given by

$$\xi(E) = \varepsilon_p(E)\,\frac{\pi a^2}{4}\,\frac{1}{\mu_m}\, e^{-\mu t}(1-e^{-\mu_m c})(1-e^{-\mu_c b})\,\frac{P_e(E)}{P_p(E)} \qquad [6]$$

$$\xi(E) = \varepsilon_\ell(E)\,\frac{\pi c}{2}\,\frac{1}{2\mu_m}\, e^{-\mu t}\,(1-e^{-\mu_m c})\,(1-e^{-\mu_c b})\, P_\ell(E) \qquad [7]$$

Note that the term $\pi c/2$ in Eqns. [3] & [7] equals half the inner circumference of the pipe and represents the width of an equivalent line source. The right hand sides of Eqns. [3] & [7] were multiplied by a factor of 0.85 to obtain agreement with experimental data.

The equations presented here were used to estimate the efficiency of a pipe source based on a measured point source efficiency. The estimated and the measured pipe source efficiencies were then compared as described below.

6.0 PIPE SOURCE EFFICIENCY - RESULTS AND DISCUSSION

Pipe source efficiencies were determined with the activity present 1) only on the internal surface of the pipe and, 2) only in the liquid. Calibration of pipe sources with surface activity only was primarily emphasized because activity of the coolant during normal PHTS operation is generally low.

Considerable delay was experienced in the fabrication of the annular uranium shield. For this reason and due to an absence of extraneous sources, all efficiency determinations in the laboratory were made using the annular lead shield previously mentioned. Performance of the uranium shield was subsequently evaluated by repeating a limited number of measurements.

As noted earlier, the efficiency determinations involved 'plug out' and 'plug in' measurements at Positions 1 and 2. Depending on peak intensities, measurements were replicated in some cases up to three times.

6.1 Surface Activity

Efficiencies were measured for two pipe sizes: Pipe 1 (ID = 7.39 cm, OD = 8.93 cm) and Pipe 2 (ID = 5.83 cm, OD = 7.27 cm). The collimator-pipe distance varied up to a maximum of 62 cm. The dimensions of collimators used are listed below; all had a hole diameter less than or equal to the diameter (2.54 cm) of the planar detector crystal.

TABLE 3

DIMENSIONS OF COLLIMATORS USED

Collimator No.	Length (cm)	Hole Dia. (cm)
2	10.16	1.27
3	10.16	1.91
4	10.16	2.54
6	6.35	1.27

Typical results are shown in Table 4. The counts in Part (a) were processed to yield the "measured" pipe source efficiency, ε, while the ε_p data was used in Eqn. [1] to determine the "calculated" ε. The remarkable agreement between the two was typical of results for both pipes at short pipe collimator distances (the R values ranged from 0.72 to 1.83).

TABLE 4
RESULTS OF A TYPICAL PIPE EFFICIENCY MEASUREMENT
(Collimator No. 4, Collimator Pipe Distance 11.8 cm, Pipe 1)

Part (a)

		Average Counts/s*			
		Position 1+		Position 2+	
Isotope	E(KeV)	Plug Out	Plug In	Plug Out	Plug In
Ce 139	166	0.3847	0.0230	0.0000	0.0000
Sn 113	392	0.2584	0.0063	0.0198	0.0055
Cs 137	662	0.9882	0.0086	0.0327	0.0371
Y 88	898	0.1664	0.0040	0.0198	0.0190
Co 60	1173	2.0479	0.2186	0.4243	0.3336
Co 60	1332	1.8998	0.2532	0.4496	0.3997
Y 88	1836	0.1083	0.0204	0.0301	0.0302

* Decay-corrected to April 27, 1987.
\+ Illustrated in Figure 8.

Part (b)

	Point Source Eff.	Pipe Eff. (Counts.cm^2/Photons)	
E(KeV)	(Counts/Photons)	Measured	Calc.
166	1.2E-03	2.5E-03	2.9E-03
392	1.9E-04	8.6E-04	8.6E-04
662	8.3E-05	4.8E-04	5.0E-04
898	5.3E-05	3.8E-04	3.7E-04
1173	3.5E-05	3.1E-04	3.0E-04
1332	2.9E-05	2.7E-04	2.6E-04
1836	1.8E-05	1.9E-04	2.0E-04

Consider the various terms in Eqn. [1]: 1) ε_p represents the point source efficiency but is measured using a source of diameter ~0.3 cm. Considering Huan's/10/ conclusion that the flux at the detector associated with an off-center point source (located anywhere within the collimator opening) is identical to that of a centered point source, the finite diameter of the point source used should be of no consequence, 2) The values used for μ, μ_m and μ_c were the commonly used "narrow beam" attenuation coefficients. The corresponding "broad beam" coefficients are expected to be lower/11/. Since "broad beam" coefficients approach "narrow beam" values with increasing thickness of the attenuation media, it is likely that the term $e^{-\mu t}$ is underestimated to a greater extent than $e^{-\mu_m c}$ and $e^{-\mu_c b}$, and 3) The

theoretical limitations on the use of Eqn. [2] to estimate P_e/P_p are best met for the smaller diameter collimators (Nos. 2 and 6); accordingly, the error in estimating P_e/P_p (Eqn. [2] underestimates it/5/) is probably the smallest for Collimators Nos. 2 and 6 and highest for Collimator No. 4. Correction for the above (Items 2 and 3) sources of error would, however, cause the value of the calculated ε to exceed the measured value.

Figure 11 shows the energy dependence of the point and pipe source efficiencies for Pipe 1 and Collimator Nos. 2-4. It is interesting to note the linearity of the pipe source efficiency plots ($\varepsilon_p(E)$ is generally linear on a logarithmic plot). The results are consistent with Eqn. [1] where the product of the exponential terms and P_e/P_p for the three collimators are essentially identical at each energy level. For Collimator No. 4 with the largest opening (a=2.54 cm), ε was greater than ε_p across the entire energy range investigated; extrapolation to lower energies suggests that ε would possibly equal ε_p at E ≈ 50 KeV. For the other two collimators, the two efficiency curves intersected within the energy range investigated with the point of intersection moving to a higher E value when "a" decreased from 1.91 cm (Collimator No. 3) to 1.27 cm (Collimator No. 2). Similar results were also obtained for Pipe 2; they are shown in Figure 12. The results are consistent with Eqn. [1] where, at each energy level, the product of the exponential terms and P_e/P_p is essentially identical for each collimator considered.

The distance dependence of the pipe source efficiency is shown in Figure 13 where the distance between collimator and pipe is expressed by the normalized factor R. As expected, the efficiency decreases with increasing distance; the decrease appears to be linear at all energy levels. Plots for the other collimators also exhibited a similar behaviour.

The ratio of the measured pipe source efficiency to that calculated based on the line source assumption (Eqn. [3]) is illustrated in Figure 14; the ratio should approach unity with increasing pipe-collimator distance. In the case of the Pipe 1 Collimator No. 2 combination, the limiting value of the ratio at large distance would probably be much less than unity except possibly at higher energies. In the case of the Pipe 2 Collimator No. 3 combination, the ratio, however, appears to be independent of photon energy and at R = 4.6 had not yet reached its limiting value. It is not evident whether at larger distances the ratio would eventually level out at unity. The reason for the different behaviours observed in the two cases examined is not clear.

6.2 Volumetric Activity

The energy dependence of the measured volumetric pipe source efficiency is shown in Figure 15 (point source efficiencies also shown for comparison) for one specific case. The dependence is linear within the limited range of photon energies investigated. Unlike the excellent agreement between experimental and calculated results for pipes with surface activity at short collimator-pipe distances, the measured volumetric efficiencies were ~63% of the calculated efficiencies from Eqn.[6].

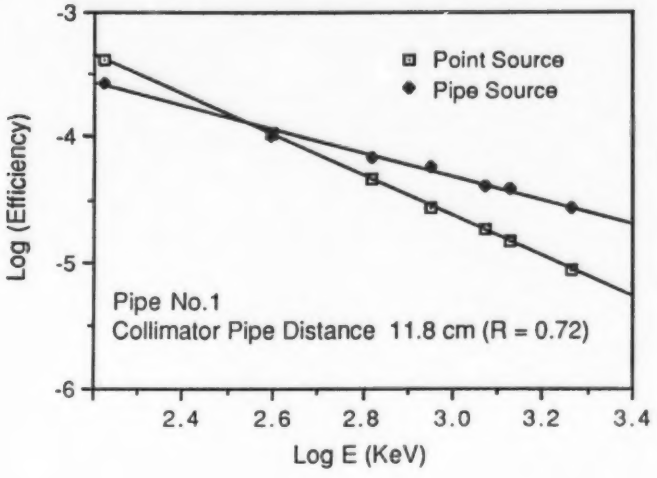

(a) Collimator No.2

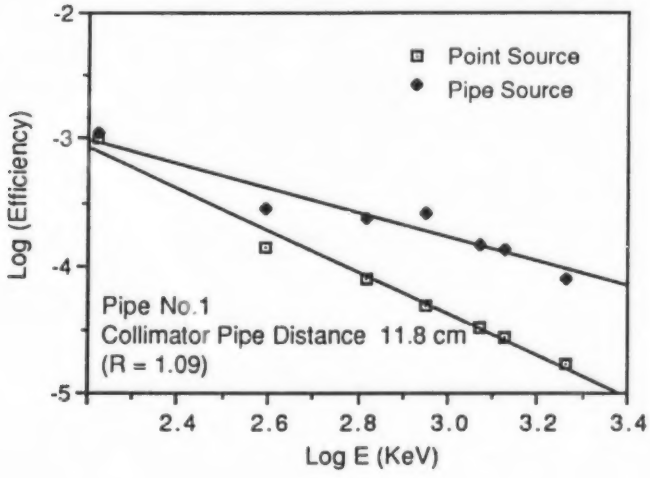

(b) Collimator No.3

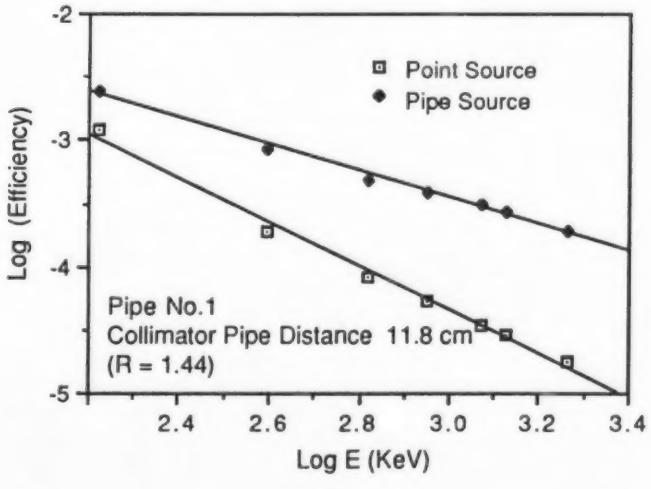

(c) Collimator No.4

FIGURE 11

ENERGY DEPENDENCE OF PIPE (SURFACE ACTIVITY) AND POINT SOURCE EFFICIENCIES - PIPE 1

178064 RD
CAZ-4

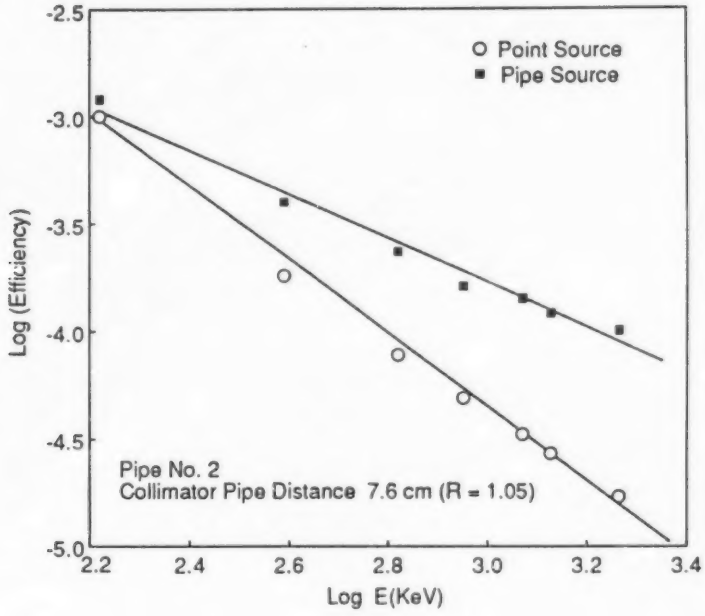

(a) Collimator No.3

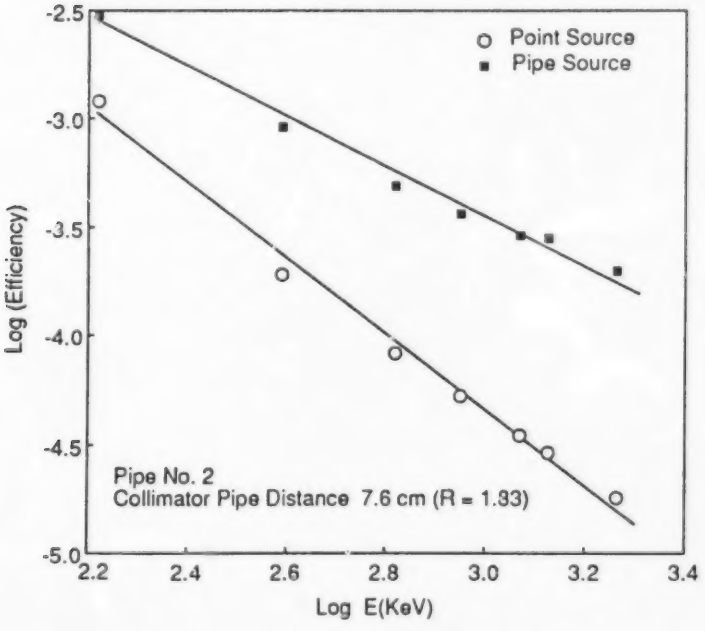

(b) Collimator No.4

FIGURE 12

ENERGY DEPENDANCE OF PIPE (SURFACE ACTIVITY)
AND POINT SOURCE EFFICIENCES - PIPE 2

177366 RD
CAZ-4

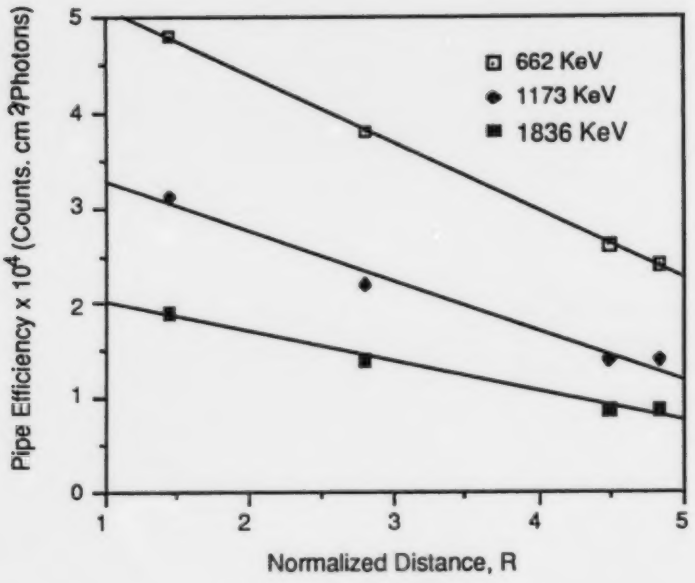

(a) Pipe 1, Collimator No.4

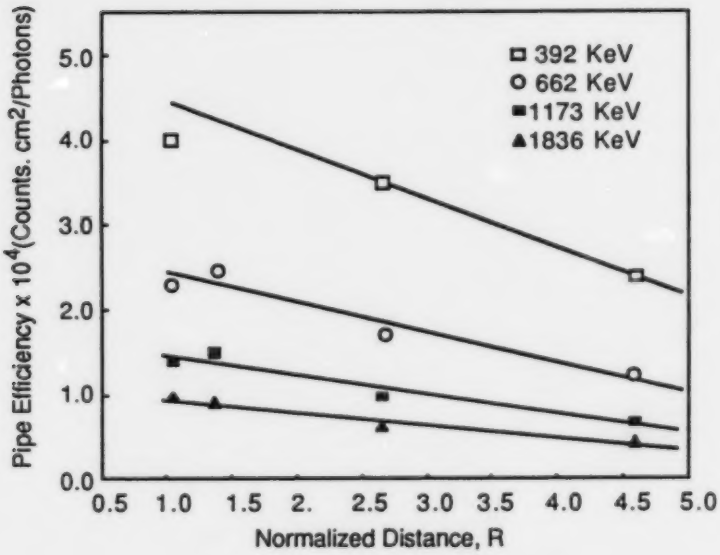

(b) Pipe 2, Collimator No.3

FIGURE 13

DISTANCE DEPENDENCE OF THE PIPE (SURFACE ACTIVITY) SOURCE EFFICIENCY

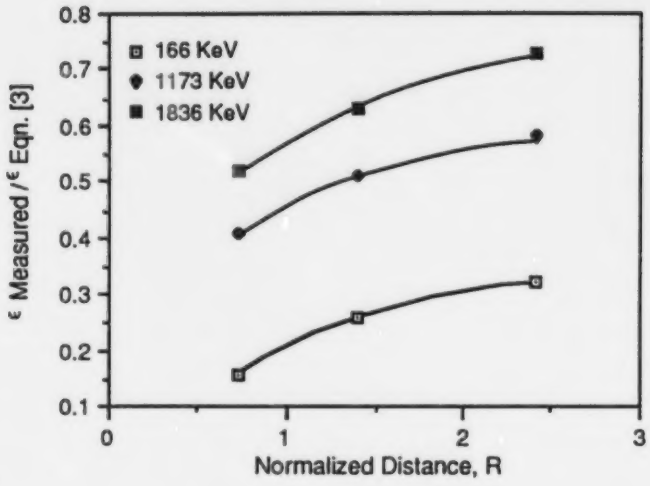

(a) Pipe 1, Collimator No.2

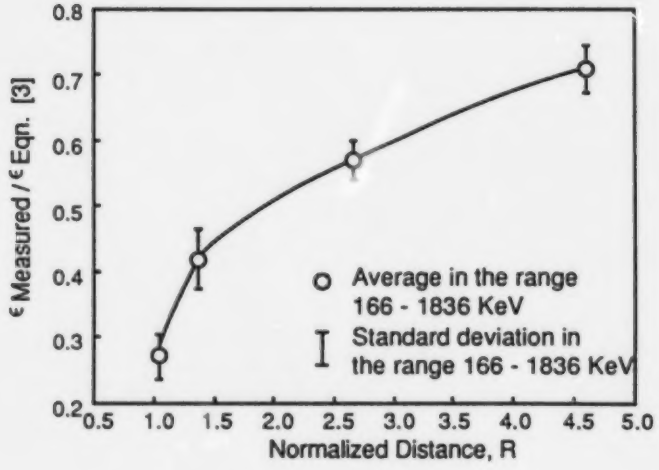

(b) Pipe 2, Collimator No.3

FIGURE 14

VARIATION WITH DISTANCE OF THE RATIO OF THE MEASURED PIPE SOURCE (SURFACE ACTIVITY) EFFICIENCY TO THAT CALCULATED BASED ON EQN. [3]

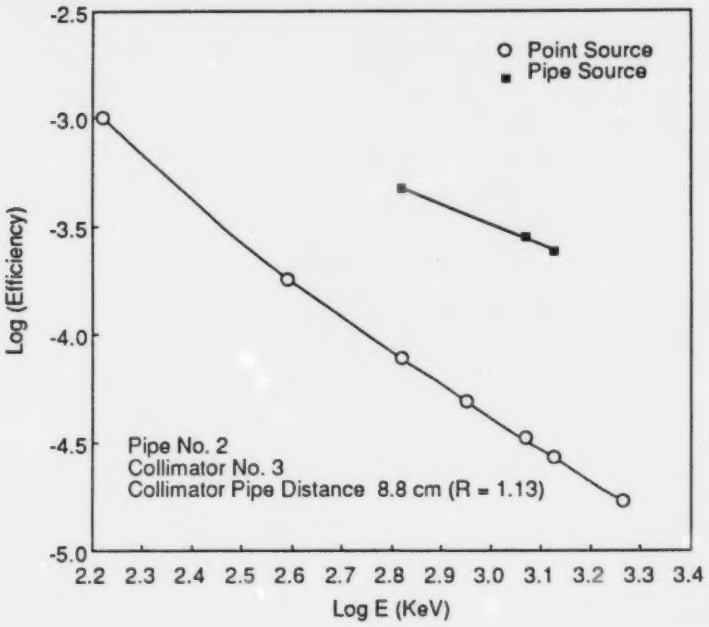

FIGURE 15

ENERGY DEPENDENCE OF PIPE (VOLUMETRIC ACTIVITY)
AND POINT SOURCE EFFICIENCIES

This is possibly due to the unexpectedly steep distance dependence of the measured efficiency at short distances (see Figure 16). In this region, the criterion $(b+D)<bc/a$ for applicability of Eqn.[6] is satisfied and theoretically the measured efficiencies are expected to be independent of distance. Possibly at distances shorter than employed in Figures 15 and 16 (ie. <8.8 cm), better agreement with theory may be realized.

The ratio of the measured pipe source efficiency to that calculated from Eqn.[7] should approach unity with increasing pipe-collimator distance. The ratios are plotted in Figure 17. As in the case of Pipe 1 with surface activity, the results suggest that a ratio of unity would be attained at a greater distance for less energetic photons. The reason for this is not clear. It appears further that the ratios would likely exceed unity with increasing distance. This is despite the fact that at these distances the criterion $(b+D)>bc/a$ is satisfied and the measured efficiencies are expected to be independent of distance.

6.3 Surface and Volumetric Activity

The distance dependences of the measured surface and volume source efficiences are compared in Figure 18 for one specific case. Since the curves are not parallel over the entire range of distances, in principle it is possible to determine the individual contributions of surface and volumetric activity of the pipe source by scanning it at a minimum of two pipe-collimator distances. This follows from the relationship

$$(\text{counts/s})_1 = \xi_1 A_v + \varepsilon_1 A_s$$
$$(\text{counts/s})_2 = \xi_2 A_v + \varepsilon_2 A_s \qquad [8]$$

where A_s and A_v denote the surface and volumetric activity, respectively, and subscripts 1 and 2 refer to the scanning distances selected.

Consider the curves in Figure 18. The preferred scanning locations were chosen to be at 7.6 cm and 62.6 cm. The pipe source efficiencies at these distances are given in Table 5. The activities of the source sheet and the liquid used to simulate a pipe with both surface and volume activity are given in Table 6. The measured counts from this pipe and the estimated activities A_s and A_v from Eqn.[8] are shown in Table 7. It is evident that for both isotopes A_s is overestimated (8-25%) while A_v is underestimated (23-40%). Despite this, the results are considered to be sufficiently encouraging to warrant a more thorough assessment of the proposed technique for measuring the contributions of surface and volumetric activities of a pipe source.

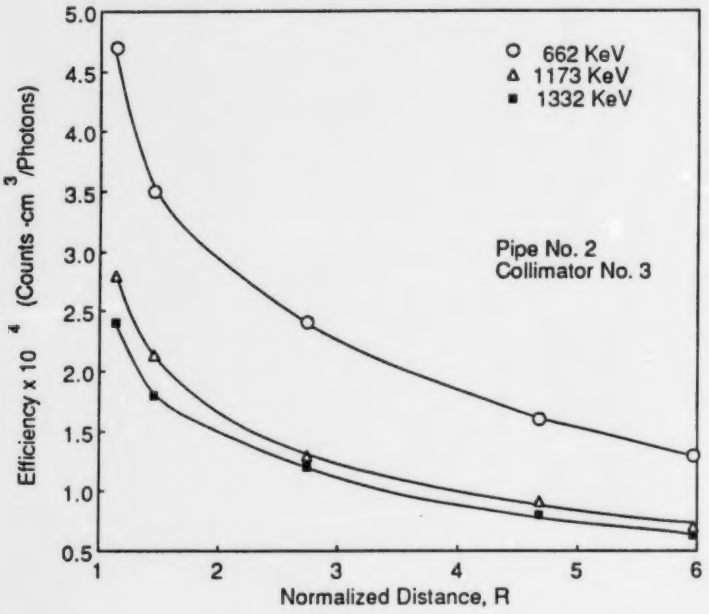

FIGURE 16

DISTANCE DEPENDENCE OF THE PIPE (VOLUMETRIC ACTIVITY) SOURCE EFFICIENCY

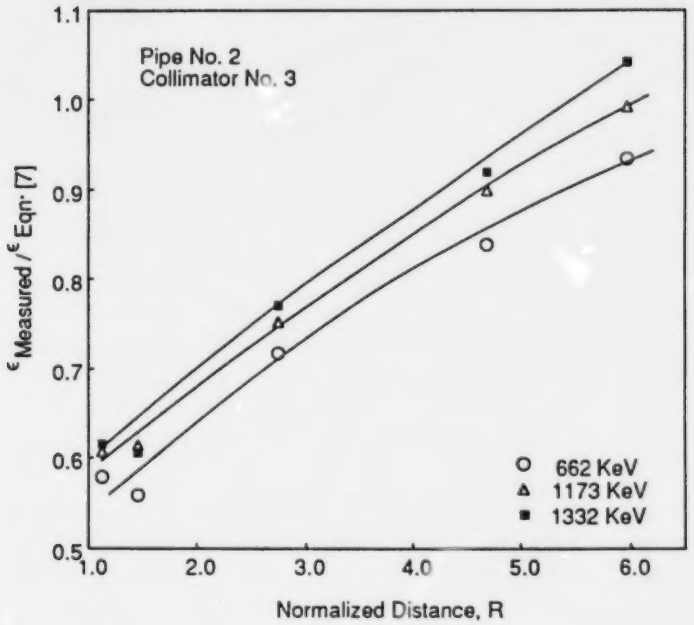

FIGURE 17

VARIATION WITH DISTANCE OF THE RATIO OF THE MEASURED PIPE SOURCE (VOLUMETRIC ACTIVITY) TO THAT CALCULATED BASED ON EQN.[7]

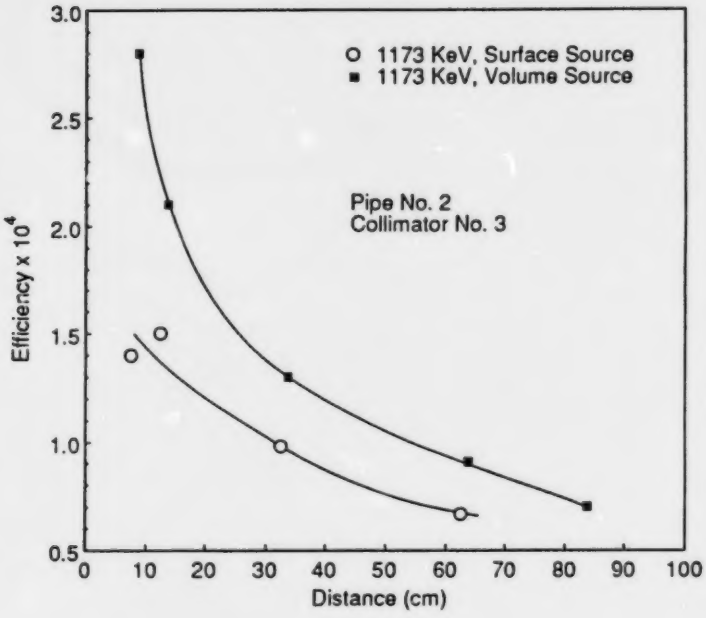

FIGURE 18

DISTANCE DEPENDENCE OF SURFACE AND VOLUME SOURCE EFFICIENCES

TABLE 5
MEASURED EFFICIENCIES FOR PIPE SOURCE
(PIPE 2, COLLIMATOR NO. 3)

Photon Energy (KeV)	ε (Counts/Photons/cm^2) 7.6 cm	ε (Counts/Photons/cm^2) 62.6 cm	ξ (Counts/Photons/cm^3) 7.6 cm	ξ (Counts/Photons/cm^3) 62.6 cm
662	2.3 E-04	1.2 E-04	4.7 E-04	1.6 E-04
1173	1.4 E-04	6.7 E-05	2.8 E-04	9.1 E-05
1332	1.2 E-04	5.7 E-05	2.4 E-04	8.0 E-05

TABLE 6
KNOWN ACTIVITIES OF PIPE SOURCE
(PIPE NO. 2)

Photon Energy (KeV)	A_s^* (Photons/s/cm^2)	A_v^* (Photons/s/cm^3)
662	4.0 E+03	4.0 E+03
1173	1.2 E+04	1.0 E+04
1332	1.2 E+04	1.0 E+04

* As on April 27, 1987.

TABLE 7
ESTIMATED ACTIVITIES OF PIPE SOURCE
(PIPE NO. 2)

Photon Energy (KeV)	Measured Counts*/s 7.6 cm	Measured Counts*/s 62.6 cm	Activity + Estimated From Eqn.[8] A_s (Photons/s/cm^2)	Activity + Estimated From Eqn.[8] A_v (Photons/s/cm^3)
662	1.162	0.489	4.5 E+03	2.8 E+03
1173	1.701	0.699	1.5 E+04	6.0 E+03
1332	1.528	0.608	1.3 E+04	7.7 E+03

* As on March 1, 1988
\+ As on April 27, 1987

6.4 Pipe Source Efficiency Calibration - Lead vs Uranium Detector Shield

As previously mentioned, the efficiency determinations in the laboratory were performed using the lead annular shield. To ascertain their applicability for interpreting field data, some of the measurements were repeated using the uranium metal shield instead. The results, given in Figure 19, indicate that with the exception of the data at 898 KeV, the efficiencies measured using the uranium shield were slightly lower than the corresponding efficiencies measured using the lead shield. Also, reproducibility of the measurements with the uranium shield was generally not as good as with the lead shield.

Despite the provision of the tungsten sleeve in the uranium shield, several peaks (identification not attempted), were observed in the spectra due to uranium decay products. In the region of interest, peaks, at 1000, 766 and 742 KeV were particularly intense. In addition to peak overlap, intensities of several peaks exceeded those of the radioisotopes in the source. To improve reproducibility, the subtraction of the 'plug in' measurement from the corresponding 'plug out' measurement was attempted using the spectra stripping function on the multi-channel analyser but to no avail; the resultant spectra, due to incomplete cancellation, still exhibited a strong presence of the peaks from the uranium shield. Although these peaks undoubtedly interferred with and complicated spectral interpretation, it is not clear whether they were responsible for the lower efficiencies measured using the uranium shield.

7.0 MEASUREMENT OF PIPE ACTIVITY - FEEDER PIPE SECTIONS

Several active feeder pipe sections from reactors at Pickering and NPD were available for direct assessment of the pipe source efficiency calibration procedures described earlier. The feeder pipes examined are listed below:

TABLE 8

ACTIVE FEEDER PIPES EXAMINED

No	Origin of Feeder Pipe	Diameter (cm) ID	Diameter (cm) OD	Contact Gamma Field* (mR/h)
1	PNGS U1 V6 Outlet	4.91	6.19	1.3
2	PNGS U2 V6 Inlet	3.75	4.95	240
3	PNGS U2 V17 Outlet	4.88	6.18	25
4	NPD A7 Inlet	3.69	4.80	80
5	NPD G7 Inlet	3.84	4.86	6

* Measured on May 29, 1986.

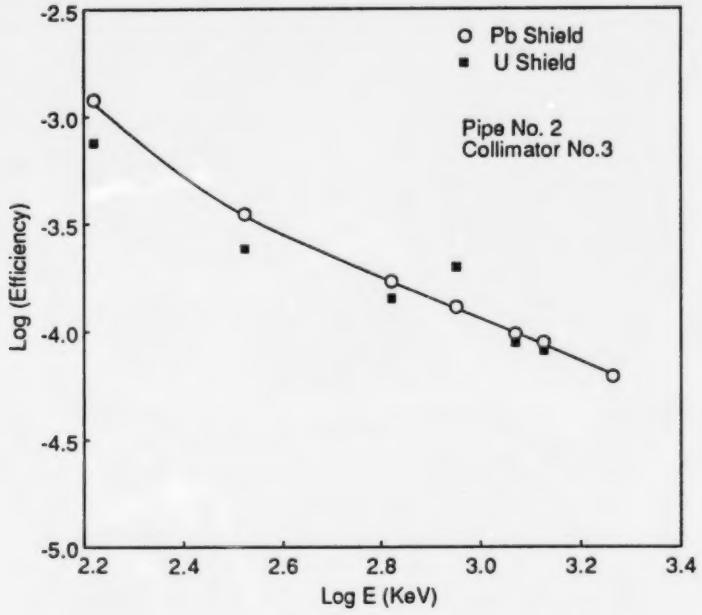

(a) Collimator Pipe Distance 32.6 cm

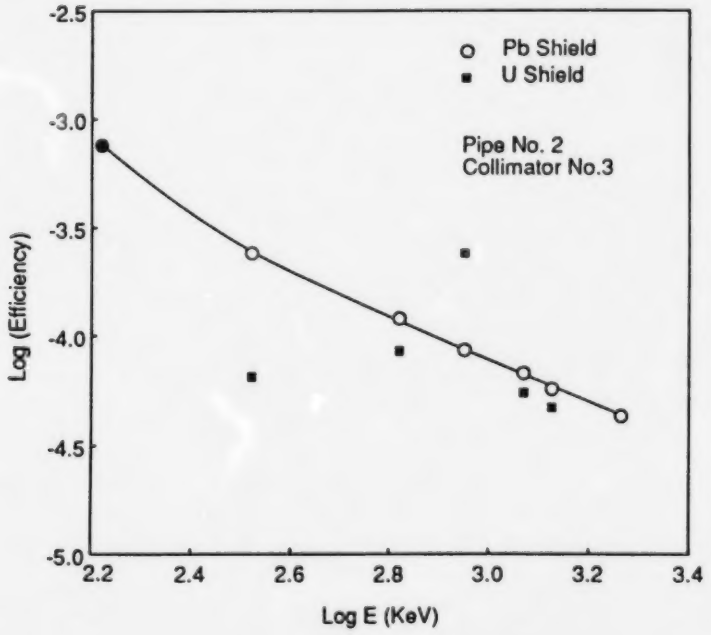

(a) Collimator Pipe Distance 62.6 cm

FIGURE 19

COMPARISON OF PIPE SOURCE (SURFACE ACTIVITY) EFFICIENCIES - LEAD VS. URANIUM DETECTOR SHIELD

177367 RD
CAZ-4

The pipes due to their short lengths were scanned only in contact with the face of the collimator. For this geometry, the detector's efficiency is well represented by the parallel plate model as previously discussed. Equation [1] applied to an empty pipe (the pipes were scanned empty) reduces to

$$\varepsilon(E) = \varepsilon_p(E) \frac{\pi a^2}{2} e^{-\mu t}(1-e^{-\mu_c b}) \frac{P_e(E)}{P_p(E)} \qquad [9]$$

This equation was used to convert the measured peak counts into the corresponding activity (Method 1). Following the pipe scans, two 2.5 cm x 2.5 cm specimens were removed from each feeder pipe for direct assay (Method 2). The specimens represented the front and the back portions of the pipes that were in the detector's field of view during the in-situ measurements.

Results from Methods 1 and 2 are compared in Table 9 (aside from Co-60, the only other significant radioisotope present was Sb-125). In general, the results obtained by Method 1 are systematically higher (up to 30%) than those based on Method 2. The systematic discrepancy probably arises, as previously discussed, from the use of "narrow beam" attenuation coefficients in Eqn. [9] and the estimation of P_e/P_p using Eqn. [2]. Taking these errors into account would yield a higher value for ε (Eqn. [9]) and hence decrease the estimated activity.

TABLE 9

ACTIVITY OF FEEDER PIPES - METHODS 1 AND 2 COMPARED

	Activity* (mCi/m^2)			
	Co-60		Sb-125	
Pipe No	Method 1+	Method 2	Method 1+	Method 2
1	0.033	0.033	0.071	0.067
2	32	28	0.513	0.450
3	3.6	3.0	-	-
4	13.3	10.2	-	-
5	1.08	0.97	-	-

* Decay-corrected to April 27, 1987.
\+ Using Collimator No. 6.

8.0 MEASUREMENT OF PIPE ACTIVITY IN FEEDER CABINET

The spectrometer system described in Section 3 was field-tested in the East feeder cabinet at Bruce Unit 1 on Feb. 27, 1987 and in the East feeder cabinet at Pickering Unit 6 on October 7, 1987.

At Bruce, the selected feeder pipe designated V14 (OD 8.94 cm and ID 7.42 cm) was connected to the inner inlet header (see Figure 1) and located near the access door. Its unshielded contact field was 250 mR/h. The spectrometer was located at an angle across the walkway with the back of the detector (shielding was lowest in this direction) facing the doorway to minimise entry of radiation to the detector from behind. In this position, the front of the equipment experienced a general radiation field of 100 mR/h while its back was exposed to a significantly lower field. Measurements were made with Collimator No. 3 at the nearest possible distance of 58 cm from the pipe. The alignment of the pipe and pipe shield with the axis of the collimator determined to a large extent the overall set-up time. A light source placed centrally in the annular shield was used for system alignment.

The only isotope detected was Co-60. The net Co-60 peak counts measured at 1173 and 1332 KeV were 1.66 cps and 1.49 cps, respectively, which corresponded (based on measured efficiencies in Section 6) to an average activity of 5.1 mCi/m^2 (volumetric activity was assumed to be negligible*).

The measured activity is probably an over-estimate due to a contribution from neighbouring pipe sources. The latter occurred because at the distance of measurement, the projection of the collimator at the plane of the pipe shield exceeded the diameter of the shield. At the risk of increased background counts, orienting the spectrometer perpendicular to the walkway would have minimised the effect of the extraneous pipe sources. However, a second set of scans could not be accommodated in the available time.

At Pickering, the selected feeder pipes designated W13 (OD 7.71 cm and ID 6.29 cm) and Q13 (OD 8.94 cm and ID 7.42 cm) were connected to the outlet header. Both pipes are located in Row E with W13 being the extremity pipe and Q13 being located immediately in front of the access door. The fields (unshielded) in contact with W13 and Q13 were 55 and 50 mR/h, respectively. The spectrometer was located perpendicularly across the walkway at both locations. The scans were made with the face of the collimator (No. 3) in contact with W13 and at ~15 cm from Q13. A telescopic rod mounted centrally inside the shielding cavity was used for alignment of the spectrometer system.

The isotopes detected and their activities determined using efficiencies calculated according to Eqn. [1] are shown in Table 10 (volumetric activity assumed negligible). Note the variability in activities of the two feeders. The peak counts were determined both by subtracting 'plug in' peak counts

* Considering a volumetric efficiency of $\approx 10^{-4}$ counts/photons/cm^3, the activity of Co-60 in the coolant (<1 μCi/kg/12/) would account for less than 0.01 cps of the measured value.

from the 'plug out' peak counts as well as by interpreting the spectrum obtained by subtracting the 'plug in' from the 'plug out' spectra. Some inconsistency was noted in Co-60 and Zr-95 activities determined by the two methods. Results from either method giving similar activity levels at two energy levels for each isotope (1173 and 1332 KeV for Co-60 and 724 and 756 KeV for Zr-95) were selected.

The experimental technique can be validated by comparing the calculated radiation doses (from measured activities) with measurements using a shielded gamma survey probe. The measured doses 250 mR/h for V14, 55 mR/h for W13 and 50 mR/h for Q13 were, however, made using an unshielded Scintrex gamma survey probe. Therefore, a direct comparison as suggested above is not possible in this instance. The shielded probe measurements for V14, W13 and Q13 can be expected to be much smaller than the corresponding unshielded probe measurements due to shine effects from neighbouring pipes. Further, the contribution of shine to the measurement is probably considerably exaggerated because of the directional dependence of the probe - the sides are up to 40% more sensitive to radiation than the front (instrument is front end calibrated).

It follows from the above that calculated doses for V14, W13 and Q13 should be significantly smaller than their measured fields of 250, 55 and 50 mR/h, respectively. This was indeed found to be the case. Calculations (performed using MICROSHIELD/13/ assuming a pipe source on contact is equivalent to two infinite parallel plane sources) suggested contact fields of 98, 23 and 8 mR/h for the three feeder pipes, respectively. Shine effects thus accounted for ~60% of the measured fields in the case of V14 and W13 and ~80% in the case of Q13.

It is concluded from the foregoing that the measured pipe activities appear to be reasonable. Quantitative verification would, however, require shielded gamma survey probe measurements to be performed in the future along with pipe spectrometry.

TABLE 10

MEASURED ACTIVITIES OF OUTLET FEEDERS IN PNGS UNIT 6

Isotope	Feeder Pipe Activity (mCi/m^2)	
	W13	Q13
Cs-137	0.05	-
Zr-95	0.59	-
Nb-95	1.10	0.95
Mn-54	0.06	-
Fe-59	0.36	-
Co-60	0.40	0.11

9.0 SUMMARY, CONCLUSIONS AND RECOMMENDATIONS

A gamma spectrometer system was developed for in-situ measurement of radioactivity within feeder pipes located in the feeder cabinets at Pickering and Bruce. Appropriate shielding was devised from a consideration of the relatively high radiation fields and multiplicity of extraneous sources at the measurement location.

The energy and distance dependence of the detector's efficiency for a pipe source with surface or volumetric activity was measured and compared with model predictions. The distance dependence of the measured efficiencies was such as to permit a determination of surface and volume contributions to the total activity of a pipe source by performing scans at two selected pipe-collimator distances. In-situ measurements of active pipe sections compared reasonably well with direct assay of appropriate specimens from the pipe sections.

The spectrometer system functioned as expected during field evaluations, ie, source counts were distinguished from background counts in fields as high as 100 mR/h. It appears, therefore, that the shielding provisions made are adequate. It would be preferable for interpreting spectra, however, to replace the annular uranium shield with one fabricated to the same specifications from tungsten alloy. The lower weight of the tungsten shield would contribute to increased portability and despite its lower attenuation, the shield would still be adequate for its intended service.

Additional measurements (including field measurements using a shielded gamma survey probe) are required to validate the proposed technique for determining feeder pipe activity.

ACKNOWLEDGEMENT

The experimental work was performed by D. Beaudry. His contribution is gratefully acknowledged.

Approved by:

D.J. Dodd
Manager
Chemical Research Department

Prepared by:

A. Husain
Engineer
Materials Chemistry Section

Reviewed by:

P. Spekkens
Program Manager
Decontamination Development

R.W. Glass
Supervising Chemist
Materials Chemistry Section

AH:dw

REFERENCES

1. SPEKKENS, P., "Contribution of Cobalt-60 to Pickering NGS Unit 1 Boiler Fields", Ontario Hydro Research Division Report No. 78-62-K.

2. SPEKKENS, P., "Shielding and Buildup Calculations for Bruce NGS Boilers", Ontario Hydro Research Division Report No. 79-251-K.

3. DORAN, F.W., "Boiler Dose Rate", Memorandum to Dyne, F.J., File 66-01133 (April 17, 1973).

4. BURRILL, K.A. and LISTER, D.H., "Radiation Field Calculations for CANDU Boilers: Self Shielding Calculations", Memorandum to Activity Transport Modelling Group" (May 13, 1977).

5. PALINO, G.F., "Radioisotope Activities on BWR Primary System Piping Part I. Calibration of the G.E. Ge(Li) Pipe Gamma Scanning System", NEDC-12646-1 (May 1977).

6. HARVILL, J.P., CORBETT, J. and BERGMANN, C.A., "Portable Monitor for the Determination of Reactor Coolant Surface Radionuclide Activities", EPRI Report, NP-2523 (July 1982).

7. ROCKWELL, T., "Reactor Shielding Design Manual", USAEC, 1st Edition, TID-7004 (1956).

8. MATHER, R.L., "Gamma-Ray Collimator Penetration and Scattering Effects", J. Applied Physics 28(10), 1200-1207 (1957).

9. POLYAKOV, V.I. and CHECHETKIN, Y.V., "Determination of the Specific Activity of γ-Emitting Isotopes in Extended Sources Without Sample Collection", Translated from Atomnaya Energiya 31(2), 139 (Aug 1971).

10. HUAN, L., "Edge Penetration by Radiation Through a Collimation System", Nuclear Instrument and Methods 197, 411-416 (1982).

11. FANO, U., "Gamma-Ray Attenuation Part II Analysis of Penetration", Nucleonics 11(9), 55-61 (1953).

12. KOS, D., "PHT Water Samples From Bruce NGS-1", Ontario Hydro Research Division, Analytical Services Section Report No. CE-88-2498-K.

13. Microshield, Version 3, Oct. 1987, Grove Engineering, Inc., Rockville, MD.